Available online at www.sciencedirect.com
ScienceDirect
Ceramics International 35 (2009) 205–211
CERAMICS INTERNATIONAL
www.elsevier.com/locate/ceramint

Effect of porosity on the elastic properties of porcelainized stoneware tiles by a multi-layered model

Valeria Cannillo [a], Leonardo Esposito [b], Elisa Rambaldi [b], Antonella Sola [a,*], Antonella Tucci [b]

[a] *Dipartimento di Ingegneria dei Materiali e dell'Ambiente, University of Modena and Reggio Emilia, Via Vignolese 905, 41100 Modena, Italy*
[b] *Centro Ceramico Bologna, Via Martelli 26, 40138 Bologna, Italy*

Received 1 August 2007; received in revised form 2 September 2007; accepted 3 October 2007
Available online 8 December 2007

Abstract

Porcelainized stoneware represents a leading product in the world market of ceramic tiles, thanks to its relevant bending strength (with respect to other classes of tiles) and extremely low water absorption: these properties derive from its really low content of residual porosity. Nevertheless, an accurate investigation of the cross section of a porcelainized stoneware tile reveals a non-uniform distribution of the residual pores through the thickness, which results in a spatial gradient of properties. Porcelainized stoneware, therefore, may be looked at as a functionally graded material. In the present research, commercial porcelainized stonewares were analysed in order to define the effect of the residual porosity and its spatial distribution on the mechanical properties of tiles. Polished cross sections of porcelainized stoneware tiles were investigated by optical and scanning electron microscopy in order to define the content and distribution of residual pores as a function of distance from the working surface. For each porcelainized stoneware, the local elastic properties of the ceramic matrix were measured by a depth-sensing Vickers micro-indentation technique, then the so-obtained microstructural images and elastic properties were used to model the stoneware tile mechanical properties. In particular, the cross section of each tile was described as a multi-layered system, each layer of which was considered as a composite material formed by a ceramic matrix and residual pores. The elastic properties of each layer were predicted by applying analytical equations derived from the theory of composite materials and, as a new approach, by performing microstructure-based finite element simulations. In order to validate the proposed multi-layered model and identify the most reliable predictive technique, the numerical results were compared with experimental data obtained by a resonance-based method.

Keywords: B. Microstructure-final; B. Porosity; C. Mechanical properties; Porcelainized stoneware

1. Introduction

Nowadays porcelainized stoneware tiles are successfully used in several building applications, both indoor and outdoor, due to their physical–mechanical performances (such as high compactness, good flexural strength, wear resistance and surface hardness), coupled with interesting aesthetic properties [1]. These performances are directly correlated to the microstructure constituted by a rather dense material in which crystals of quartz and mullite are dispersed in a large amount of glassy matrix. In fact the maximum temperature reached during firing, 1210–1230 °C, accomplishes the sintering and significantly reduces the total porosity.

Even if these tiles exhibit a negligible water absorption (usually lower than 0.5%: group BIa of ISO 13006 [2]), which is due to a near-zero open porosity [3,4], they retain a noticeable closed porosity, reaching also values as high as 6.0% [5]. On the basis of these observations, porcelainized stoneware is a ceramic body constituted by a material core characterised by a not negligible porosity, completely surrounded by a thin and almost impervious surface layer. This non-homogeneity can be easily detected after polishing [6] and/or analysing by light microscopy the cross section of suitable specimens polished to mirror like.

* Corresponding author. Tel.: +39 059 2056281; fax: +39 059 2056243.
E-mail address: sola.antonella@unimore.it (A. Sola).

0272-8842/$34.00
doi:10.1016/j.ceramint.2007.10.015

Even if the relation between porosity and elastic properties was intensively investigated in the past [7–10], until now very little attention was addressed to the dependence of the mechanical behaviour of ceramic tiles on the porosity content and spatial distribution; in particular, little scientific attention was paid to porcelain stoneware tile properties [4]. The present work investigates the effect of the residual porosity on the elastic properties of commercial porcelainized stoneware tiles, by applying a multi-layered model inspired by the research field of functionally graded materials.

2. Materials and methods

2.1. The multi-layered model

In order to evaluate the effect of the total residual porosity and its distribution on the material behaviour and to apply the multi-layered model, the following hypotheses were set:

- The porosity content is uniform in each plane parallel to the working surface; in other words, it only depends on the distance from the external surfaces. This assumption is based on the geometry of tiles, which is substantially planar. Moreover, the typical processing of porcelainized tiles mainly consists of two steps: (i) uniaxial pressing of the pre-mixed spray-dried raw materials and (ii) a very fast firing cycle, during which the heat exchange mainly occurs through (and perpendicular to) the back and the working surfaces [11].
- The porcelainized stoneware may be regarded as a biphasic composite material, in which the residual porosity is dispersed in a ceramic matrix.
- The ceramic matrix is assumed to be uniform. As a matter of fact, the final product consists of a glassy matrix with a feldspathic nature, containing crystalline phases such as quartz and mullite [3,4]. In the present research, however, the matrix is modelled as a homogeneous ceramic material, disregarding chemical and mineralogical variations, in order to stress the role of porosity on the porcelainized stoneware performances.

Based on these assumptions, a porcelainized stoneware tile may be considered as a unidirectional functionally graded material, since the volume fractions of the constituent phases – the dispersed residual pores and the continuous ceramic matrix – vary as a function of thickness, i.e. distance from the working surface [12]. In order to simplify the analysis, the material is modelled as a multi-layered system, or a stack of perfectly bonded sub-layers, each is described as a uniform composite material. In the multi-layered approach, therefore, a step-wise compositional change approximates the actual continuous variation. The main advantage of the multi-layered approach is that each sub-layer may be investigated as a traditional composite material and constitutive laws may be used to predict its properties [12]. It is worth noting that the multi-layered model is effective only if the thickness of each sub-layer is greater than the characteristic microstructural unit size (e.g. average pore size [12,13]). However the number of layers should be high enough to provide a reliable description of the gradient of properties in the analysed system.

Table 1
Chemical composition of the tested samples (wt.%)

	PS1	PS2
Na_2O	5.20	2.99
MgO	0.58	0.83
Al_2O_3	19.55	19.28
SiO_2	70.13	72.44
K_2O	2.43	2.84
CaO	0.73	0.61
TiO_2	0.94	0.52
Fe_2O_3	0.44	0.49

Table 2
Quantitative mineralogical composition of the tested samples (wt.%)

	PS1	PS2
Quartz	24.2 ± 0.2	14.2 ± 0.2
Mullite	4.2 ± 0.4	4.4 ± 0.5
Plagioclase	–	4.1 ± 0.4
Zircon	–	3.4 ± 0.1
Glassy phase	71.6 ± 1.1	73.9 ± 1.7

2.2. Materials

In the present work two industrial porcelainized stonewares, PS1 and PS2, were investigated. Their chemical and mineralogical compositions are shown in Tables 1 and 2, respectively. The chemical analyses were performed by microanalysis SEM-EDS (Zeiss EVO 40, D and Inca, Oxford Instruments, UK) and the quantitative mineralogical compositions were determined by X-ray diffraction analysis (PW3830, Philips, NL). Powdered specimens, diluted with 10 wt.% of corundum NIST 676 as internal standard, were side loaded to minimize preferred orientation. Data were collected in the angular range 10–80° 2θ with steps of 0.02° and 5 s/step and the Rietveld refinements were performed using GSAS [14].

For each material, the tile was ideally subdivided into 12 layers. The thickness of the first layer was set to 50 μm, in order

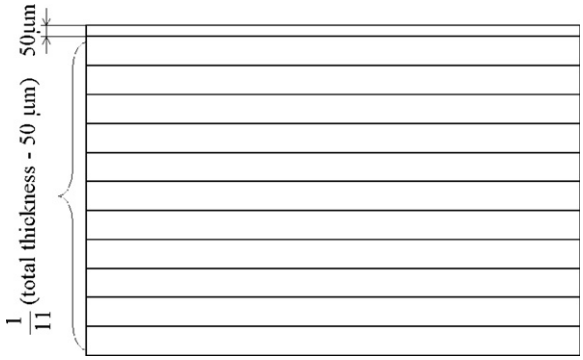

Fig. 1. Schematic drawing of the multi-layered model used to describe a porcelainized stoneware tile.

to account for the near-zero superficial open porosity; instead, the remaining eleven layers had the same thickness (about 700 μm each), as schematically shown in Fig. 1.

2.3. Porosity evaluation

In order to evaluate the pore amount as a function of distance from the working surface, optical microscope images were considered. For both materials, polished cross sections were observed with an optical microscope and the objective 10× was used to collect at least five images for each layer; the contrast was purposely enhanced to reveal the pores. The area occupied by the pores was quantified by means of image analysis software (UTHSCSA Image Tool); the average porosity was successively calculated within each layer.

Then, for each layer, a representative image acquired by the optical microscope was chosen and used for subsequent elaboration. In particular, for each layer, the porosity calculated in the selected picture was as close as possible to the average porosity of the respective layer (Fig. 2).

2.4. Elastic properties evaluation

With the aim of estimating the elastic properties as a function of depth, three different equations relating Young's modulus with porosity were applied to the twelve representative microstructural images (acquired by optical microscope) of each porcelainized stoneware.

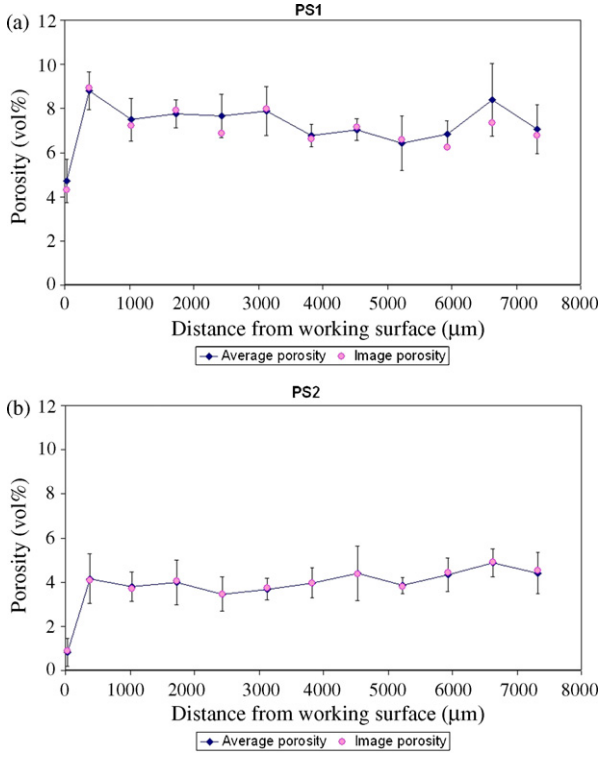

Fig. 2. Average porosity as a function of distance from the working surface and porosity of the representative images (used to evaluate the elastic properties) in PS1 (a) and PS2 (b).

The Voigt equation corresponds to an upper bound [7]. Though originally developed for the shear and bulk moduli [7], it is quite often applied directly to the Young's modulus [15,16]. Since the system in question here is a biphasic composite material and the void phase shows zero properties from a mechanical point of view [7,8], the Voigt equation reduces to the relation:

$$E_V = E_0(1 - p) \tag{1}$$

where E_V is the tensile modulus of the porous material, E_0 is the tensile modulus of the pore-free matrix and p is the porosity (expressed as a fraction).

The Hashin–Shtrikman (HS) relations represent accurate bounds for the elastic (specifically, bulk and shear) moduli of macroscopically isotropic biphasic composites [7]. If the pores are one of the two constituent phases, the HS lower bounds degenerate to zero, while the HS upper bounds are described by the following relations [7]:

$$\frac{G_{HS}}{G_0} = 1 - p\left[\frac{15\,K_0 + 20\,G_0}{9\,K_0 + 8\,G_0 + (6\,K_0 + 12\,G_0)\,p}\right] \tag{2}$$

$$\frac{K_{HS}}{K_0} = 1 - p\left[\frac{3\,K_0 + 4\,G_0}{3\,K_0\,p + 4\,G_0}\right] \tag{3}$$

where G_{HS} and K_{HS} are the predicted upper bounds for the shear and the bulk moduli of the porous material, G_0 and K_0 are the elastic moduli of the matrix and, as previously set, p is the porosity. The respective bound for the Young's modulus E_0 of the porous material can be inferred by the expression [7]:

$$E_{HS} = \frac{9K_{HS}\,G_{HS}}{3K_{HS} + G_{HS}} \tag{4}$$

The Spriggs equation [8], or exponential equation (5), is widely used to predict the Young's modulus of porous biphasic systems [8,10]:

$$E_S = E_0\,e^{-b\,p} \tag{5}$$

being E_S the predicted Young's modulus of the porous material, E_0 the elastic modulus of the pore-free matrix and b an empirical constant, which should be calculated by fitting experimental data. As a matter of fact, the constant b depends on the fabrication technique and, according to Spriggs [9], perhaps on the type of material and measurement technique. However, for porcelainized materials having a pore size smaller than 80 μm, a value of 2.96 may be used for the parameter b [8].

Besides the analytical equations, the elastic modulus of the porcelainized stoneware tile was evaluated as a function of the distance from the working surface by means of a computational approach. The simulations were performed by using OOF (Object-Oriented Finite element method) [17,18], a software which is able to apply the finite element method (FEM) at the microscale. In fact, it can read digitalized images of the real microstructure and assign materials properties to features in the picture. The image is directly mapped onto a two-dimensional finite element mesh and used to perform virtual experiments. Since the computer simulations are based on actual microstructure and materials properties, OOF can be used to

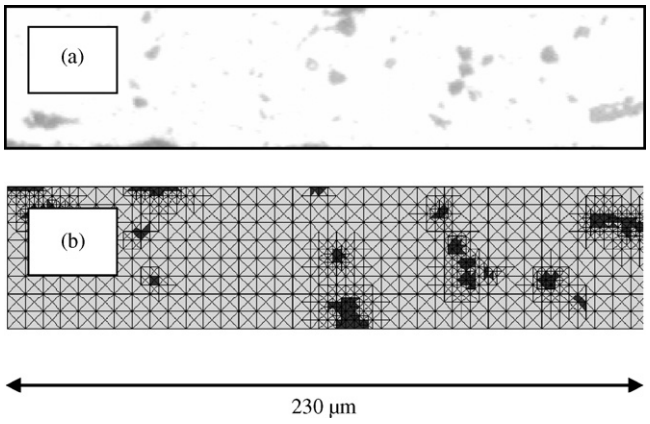

Fig. 3. Example of a microstructure-based finite element mesh referring to a detail of the first layer in PS1: microstructural image (a) and respective grid (b). In light gray: ceramic matrix; in dark gray: pores.

investigate the relationship existing between microscopic geometry and overall microscopic performances. Thanks to its flexibility, this code can be used to study also complicated systems, such as composites and functionally graded materials and several aspect of materials behaviour can be considered: elastic properties, fracture mechanics, thermal conductivity, and piezoelectricity [19–35].

For both PS1 and PS2, OOF was applied to the twelve selected pictures of the tile cross section, which were mapped onto 2D finite element meshes, as shown in Fig. 3. A constant number (96,000) of triangular elements was used for comparison purposes. In order to evaluate the elastic properties, a tensile test was simulated on each mesh. A fixed strain was imposed along the "y" direction (parallel to the tile thickness) to obtain E_y and the virtual test was repeated applying a strain along the "x" direction (parallel to the working surface) to evaluate E_x. The input data (properties of the constituent phases) are listed in Table 3.

In particular, the elastic modulus of the pore-free ceramic phase (also used as E_0 in the analytical equations) was obtained via a depth-sensing Vickers micro-indentation technique. The indentation method basically consists of two steps. In the first step, the indenter tip (a Vickers one in the present research) penetrates into the material while the applied load is progressively increased to its maximum value. In the second step, the load is removed and the indenter is moved upward. Both the loading and the unloading rates are constant. During the two steps of the indentation, the applied load and the corresponding penetration depth are registered. Even if during the indentation the material behaviour depends on both its elastic and plastic properties, a proper analysis of the unloading part of the load–

Table 3
Main mechanical properties of the constituent phases

	Young's modulus (GPa)	Poisson's coefficient
PS1, matrix	102 ± 8	0.23 [9]
PS2, matrix	93 ± 9	0.23 [9]
Pores	0	0

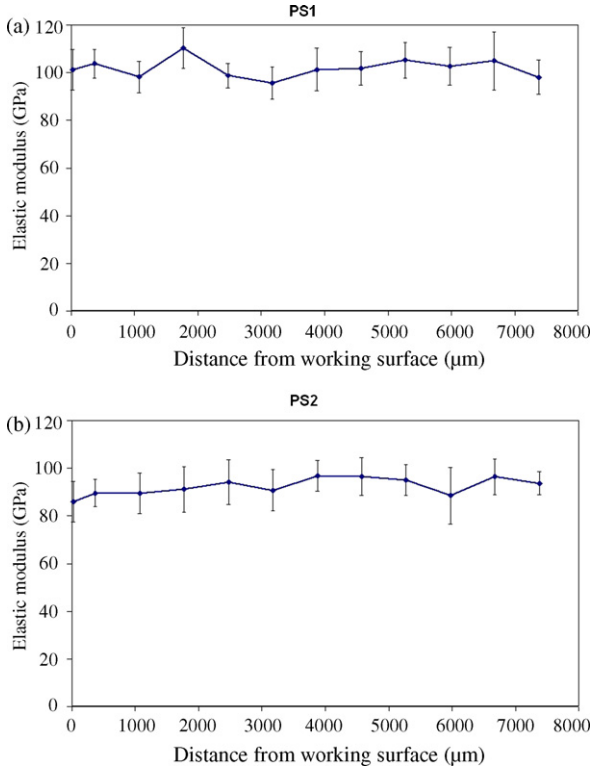

Fig. 4. Young's modulus as a function of distance from the working surface as measured by depth-sensing micro-indentation in PS1 (a) and PS2 (b).

displacement curve, which represents the relaxation of the elastic deformation, makes it possible to evaluate the elastic modulus of the material [36]. Various methods have been proposed to analyse the unloading curve [36], but the one proposed by Oliver and Pharr [37] is the most frequently used, since it describes the first portion of the unloading curve by a relatively simple power law equation and usually gives reliable results [37]. In the present investigation, for both porcelainized stonewares, a set of indentions was carried out on the tile cross section (at least five valid indentations within each layer; maximum applied load: 1 N; loading/unloading rate: 2 N/min) and, for each indentation, the elastic modulus was deduced from the load–depth curve by the Oliver–Pharr method [37]. As shown in Fig. 4, the average elastic modulus was calculated within each layer but it was not possible to observe a significant correlation between elastic modulus and depth ("y" coordinate). Since the indentations were performed on pore-free areas and the measured elastic modulus did not depend on depth, the homogeneity of the matrix was confirmed (at least from a mechanical point of view) and the collected values could be used to evaluate, through the thickness, the average elastic modulus of the pore-free ceramic matrix.

For each porcelainized stoneware the overall elastic modulus (porosity included) was experimentally measured via a resonance-based technique (EMOD, Lemmens Grindosonic® MK5) on at least 5 bars (70 mm × 22 mm × 8 mm). The result could be considered as the elastic modulus of the system (matrix + pores).

Even if the analytical equations and the microstructure-based finite element simulations were applied to the optical

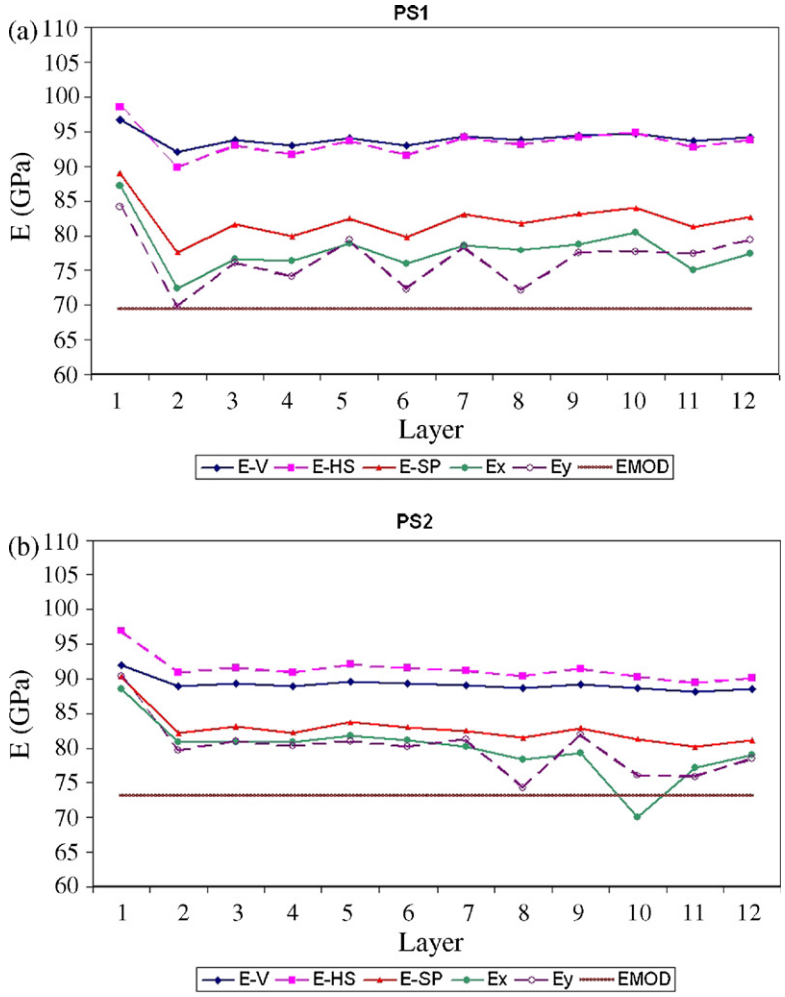

Fig. 5. Comparison between the elastic properties predicted by the FE simulation ("*X*" direction: E_x; "*Y*" direction: E_y), the analytical values (Voigt equation: *E*–*V*; HS equation: *E*–HS; Spriggs equation: *E*–SP) and the EMOD measure (EMOD) in PS1 (a) and PS2 (b).

microscope images, the microstructural features of the samples were also analysed by SEM (Zeiss EVO 40, D).

3. Results and discussion

The elastic modulus of the (pore-free) ceramic matrix of the two porcelainized stonewares, as measured by the depth-sensing micro-indentation technique, did not depend on the distance from the working surface, as shown in Fig. 4, and its average value was 102 ± 8 GPa for PS1 and 93 ± 9 GPa for PS2, as listed in Table 3.

The results of the analytical predictions, as well as the computational simulations, are shown in Fig. 5. The Young's modulus measured by the resonance-based technique, i.e. 69.4 ± 1.7 GPa for PS1 and 73.1 ± 0.5 GPa for PS2, can be assumed as a benchmark and it is also indicated in Fig. 5. However, this is just an indicative value, since it represents an average elastic modulus of the porcelainized stoneware through the thickness and it does not provide any information about the change of the elastic properties in the volume.

The values in Table 3 and the results in Fig. 5 suggest that it is extremely important to account for the effect of porosity on the mechanical properties of porcelainized stoneware tiles, since pores may significantly reduce the overall elastic modulus with respect to the pore-free ceramic matrix. For example, if compared to PS2, PS1 shows a lower overall Young's modulus as measured via the resonance-based technique, even if the Young's modulus of its pore-free ceramic matrix is higher than that of PS2. The main reason is that the residual porosity is more abundant in PS1 than in PS2, as shown in Fig. 2.

The Voigt equation implies a linear dependence of the Young's modulus on porosity: the higher the porosity, the lower the elastic modulus. As a consequence, a parallel can be drawn between the system composition and the elastic properties. In particular, in the multi-layered systems considered here, the highest modulus is achieved in the first layer, because it is particularly compact, while the lowest values are calculated in the second (PS1) and the eleventh (PS1 and PS2) layers, where the porosity is particularly abundant. All the values obtained by the Voigt equation, however, are significantly higher than the experimental information obtained by the resonance-based method, but it should be underlined that the Voigt relation provides an upper bound and not strictly a prediction.

The HS estimates are nearly coincident with the Voigt ones and therefore they also overestimate the Young's modulus of the porcelainized stonewares. As a matter of fact, the HS can be

regarded as really accurate bounds which, in the case of porous materials, give an upper limit for the elastic moduli. Moreover, the HS bounds apply to the shear modulus and to the bulk modulus; as a consequence, the corresponding value of the tensile modulus has to be indirectly deduced from additional calculations [7].

As regards the Spriggs relation, Pabst et al. [7] have recently stated that it violates the HS upper bound and it does not satisfy the boundary condition E (composite) = 0 for a porosity $p = 1$. Nonetheless, Pickup [8] has remarked that it is unlikely that a single equation would work properly on the entire range of porosity (0–1). Since the porosity of the systems considered here does not exceed 9 vol% (i.e. $p < 0.09$), it is reasonable that the exponential equation will hold. As shown in Fig. 5, the Spriggs equation emphasizes the effect of porosity on elastic properties; moreover, the values predicted by the exponential relation are significantly lower than the Voigt and the HS ones, giving a more realistic estimation of the elastic profile along the tile thickness.

Fig. 5 suggests that a parallel may be drawn between the values predicted by the computational simulations and those calculated by the Spriggs equation; nevertheless, the FEM-based estimates are much closer to the experimental (resonance-based method) value. In fact, the exponential equation (as well as the Voigt relation and the HS bounds) only deals with the porosity volume fraction and it does not include any information about the pore shape [7]. The microscale modeling, instead, relies on microstructural images and hence it takes into account the actual shape, dimension and distribution of the constituent phases. Moreover, unlike the previously described analytical equations, the finite element analysis makes it possible to study the elastic properties along different directions, by simulating tensile tests along different axes. However, as shown in Fig. 5, if a fixed distance from the working surface is considered, both the porcelainized stonewares do not exhibit different behaviours along the relevant directions considered here, i.e. the tile thickness direction y (E_y) and the in-plane direction x parallel to the working surface (E_x). In other words, the simulations show that, within each layer, the mechanical behaviour is substantially isotropic (E_x comparable to E_y). This appears reasonable, since the microstructural inspection did not reveal any preferential orientation of the residual pores and other microstructural features within each layer. However the computational simulations confirm that both E_x and E_y vary as a function of depth, as a result of the pore distribution.

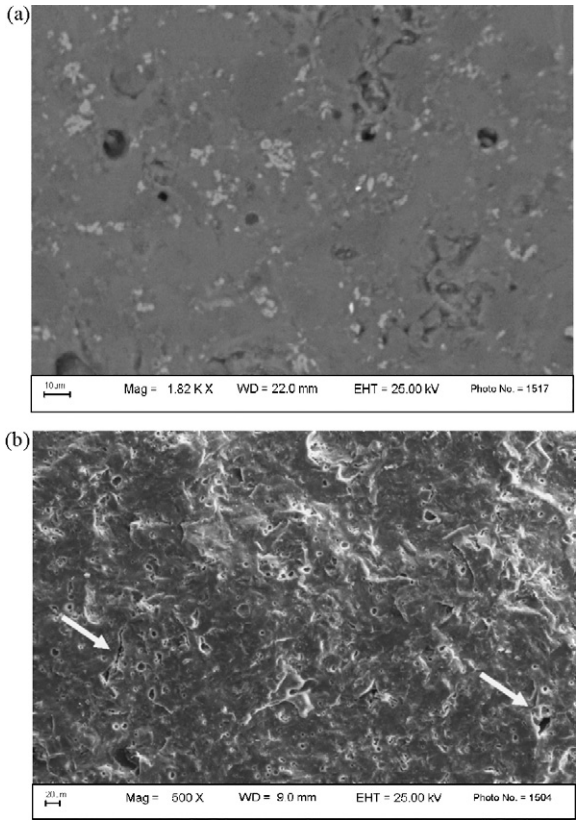

Fig. 6. SEM micrographs: (a) BEI image of polished surface of sample PS2; (b) SEI image of fractured surface in PS1, the arrows point elongated micro-flaws.

Even if the computational simulations are more reliable than the analytical equations, the FEM results still overestimate the experimental data (resonance-based method). The reason for this discrepancy may be the use of 2D images to model a 3D system. In fact the image analysis of planar sections is advantageous due to its easiness, but it furnishes indirect information on three-dimensional real microstructures [7,33]. Moreover, a microscope-acquired image is an approximation to the real microstructure and the built mesh, in its turn, is an approximation to the image [18]. In addition, the present computational simulation was based on images obtained by optical microscope that, having lower resolution and lower depth of field than SEM, is able to give less detailed but more significant information on the residual porosity on a wide range of pore size, down to 10 μm. However the model cannot include those local micro-defects and heterogeneities that, due to their thinness, are hardly detected without the help of scanning electron microscope investigation. In Fig. 6, some of these peculiarities are reported. In particular, in Fig. 6a, the BEI image of the polished surface of PS2 allows to evaluate the chemical heterogeneity of the ceramic matrix, including, for this material, also zircon (light particles) and quartz (gray particles) dispersed in an apparently homogeneous glassy phase. While the SEM analysis of the fracture surfaces (Fig. 6b) of the tested samples revealed a widespread presence of very thin elongated micro-flaws.

However it should be underlined that the analytical equations and, even more, the computational simulations based on the multi-layered model are extremely useful, since they enable to appreciate the variation of the elastic modulus as a function of the distance from the working surface inside the stoneware porcelainized tiles. This functional gradient, instead, cannot be revealed by traditional experimental techniques – such as the resonance-based method – which evaluate the average properties of the body.

4. Conclusions

As a result of the fast-firing cycles used in industrial production, porcelainized stoneware tiles may retain a not negligible residual porosity, whose distribution is not uniform through the thickness. In order to account for the dependence of

porosity on depth, a porcelainized stoneware tile can be regarded as a functionally graded material and hence it can be modelled as a multi-layered system. After evaluating the pores volume fraction as a function of the distance from the working surface, the effect of porosity on elastic properties can be appreciated by applying proper analytical equations within each layer of the material model. The Voigt equation and the Hashin–Shtrikman ones provide useful upper bounds for the elastic modulus, but a more reliable prediction can be obtained by applying the Spriggs (or exponential) equation. Nonetheless, a more accurate approach is represented by the computational simulation of the stoneware tile, which relies on the application of the finite element method to real microstructural images. The simulations confirm that the porosity distribution along the tile thickness results in a spatial variation of elastic properties, which cannot be revealed by traditional experimental methods such as flexural tests and resonance-based techniques.

Acknowledgement

Ing. Giovanni Giannini is gratefully acknowledged for his precious help.

References

[1] L. Esposito, A. Tucci, E. Rastelli, C. Palmonari, S. Selli, Stain resistance of porcelain stoneware tile, Am. Ceram. Soc. Bull. 81 (10) (2002) 38–42.
[2] International Standard ISO 13006 Ceramic tiles—definitions, classification, characteristics and marking, 1998.
[3] P.M. Tenorio Cavalcante, M. Dondi, G. Ercolani, G. Guarini, C. Melandri, M. Raimondo, E. Rocha e Almendra, The influence of microstructure on the performance of white porcelain stoneware, Ceram. Int. 30 (2004) 953–963.
[4] E. Sánchez, M.J. Ibáñez, J. García-Ten, M.F. Quereda, I.M. Hutchings, Y.M. Xu, Porcelain tile microstructure: implications for polished tile properties, J. Eur. Ceram. Soc. 26 (2006) 2533–2540.
[5] I.M. Hutchings, Y. Xu, E. Sánchez, M.J. Ibáñez, M.F. Quereda, Porcelain tile microstructure: implications for polishability, J. Eur. Ceram. Soc. 26 (2006) 1035–1042.
[6] E. Sánchez, Technical considerations on porcelain tile products and their manufacturing process. Part II, Interceramics 52 (3) (2003) 132–138.
[7] W. Pabst, E. Gregorová, G. Tichá, Elasticity of porous ceramics—a critical study of modulus–porosity relations, J. Eur. Ceram. Soc. 26 (7) (2006) 1085–1097.
[8] R. Pickup, Effect of porosity on Young's modulus of a porcelain, Br. Ceram. Trans. 96 (3) (1997) 96–98.
[9] R.M. Spriggs, Expression for effect of porosity on elastic modulus of polycrystalline refractory materials, particularly aluminum oxide, J. Am. Ceram. Soc. 44 (12) (1961) 628–629.
[10] R.A. Dorey, J.A. Yeomans, P.A. Smith, Effect of pore clustering on the mechanical properties of ceramics, J. Eur. Ceram. Soc. 22 (2002) 403–409.
[11] L. Esposito, A. Tucci, D. Naldi, The reliability of polished porcelain stoneware tiles, J. Eur. Ceram. Soc. 25 (9) (2005) 1487–1498.
[12] Y. Miyamoto, W.A. Kaysser, B.H. Rabin, A. Kawasaki, R.G. Ford, Functionally Graded Materials. Design, Processing and Applications, Kluwer Academic Publishers, 1999.
[13] A. Mortensen, S. Suresh, Functionally graded metals and metal–ceramic composites. II. Thermomechanical behaviour, Int. Mater. Rev. 42 (3) (1997) 85–116.
[14] A.C. Larson, R.B. Von Dreele, "GSAS, General Structural Analysis System", Los Alamos National Laboratory Report, LAUR, 1994, 86-748.
[15] R.F. Gibson, Principles of Composite Material Mechanics, McGraw-Hill International Editions, 1994.
[16] E.J. Barbero, Introduction to Composite Materials Design, Taylor and Francis, 1998.
[17] W.C. Carter, S.A. Langer, E.R. Fuller Jr., The OOF Manual, Version 1.0, 1998.
[18] S.A. Langer, E.R. Fuller Jr., W.C. Carter, OOF: an image-based finite element analysis of material microstructures, Comput. Sci. Eng. 3 (2001) 15–23.
[19] C.H. Hsueh, E.R. Fuller Jr., S.A. Langer, W.C. Carter, Analytical and numerical analyses for two-dimensional stress transfer, Mater. Sci. Eng. A 268 (1–2) (1999) 1–7.
[20] C.H. Hsueh, J.A. Haynes, M.J. Lance, P.F. Becher, M.K. Ferber, E.R. Fuller Jr., S.A. Langer, W.C. Carter, W.R. Cannon, Effects of interface roughness on residual stresses in thermal barrier coatings, J. Am. Ceram. Soc. 82 (4) (1999) 1073–1075.
[21] C.H. Hsueh, E.R. Fuller Jr., Residual stresses in thermal barrier coating: effects of interface asperity curvature/height and oxide thickness, Mater. Sci. Eng. A 283 (1–2) (2000) 46–55.
[22] A. Zimmermann, E.R. Fuller Jr., J. Rödel, Residual stress distributions in ceramics, J. Am. Ceram. Soc. 82 (11) (1999) 3155–3160.
[23] A. Zimmermann, W.C. Carter, E.R. Fuller Jr., Damage evolution during microcracking of brittle solids, Acta Mater. 49 (1) (2001) 127–137.
[24] M.H. Zimmerman, D.M. Baskin, K.T. Faber, E.R. Fuller Jr., A.J. Allen, D.T. Keane, Fracture of a textured anisotropic ceramic, Acta Mater. 49 (16) (2001) 3231–3242.
[25] V.R. Vedula, S.J. Glass, D.M. Saylor, G.S. Rohrer, W.C. Carter, S.A. Langer, E.R. Fuller Jr., Residual-stress predictions in polycrystalline alumina, J. Am. Ceram. Soc. 84 (12) (2001) 2947–2954.
[26] A. Saigal, E.R. Fuller Jr., S.A. Langer, W.C. Carter, M.H. Zimmerman, K.T. Faber, Effect of interface properties on microcracking of iron titanate, Scripta Mater. 38 (9) (1998) 1453–1499.
[27] A. Saigal, E.R. Fuller Jr., Analysis of stresses in aluminium–silicon alloys, Comput. Mater. Sci. 21 (1) (2001) 149–158.
[28] V. Cannillo, W.C. Carter, Computation and simulation of reliability parameters and their variations in heterogeneous materials, Acta Mater. 48 (13) (2000) 3593–3605.
[29] V. Cannillo, C. Leonelli, T. Manfredini, M. Montorsi, A.R. Boccaccini, Computational simulations for the assessment of the mechanical properties of glass with controlled porosity, J. Porous Mater. 10 (3) (2003) 189–200.
[30] V. Cannillo, C. Leonelli, A.R. Boccaccini, Numerical models for thermal residual stresses in Al_2O_3 platelets/borosilicate glass matrix composites, Mater. Sci. Eng. A 323 (2002) 246–250.
[31] V. Cannillo, A. Corradi, C. Leonelli, A.R. Boccaccini, A simple approach for determining the in situ fracture toughness of ceramic platelets used in composite materials by numerical simulations, J. Mater. Sci. Lett. 20 (2001) 1889–1891.
[32] V. Cannillo, G.C. Pellacani, C. Leonelli, A.R. Boccaccini, Numerical modeling of the fracture behavior of a glass matrix composite reinforced with alumina platelets, Composites A 34 (2003) 43–51.
[33] V. Cannillo, T. Manfredini, M. Montorsi, A.R. Boccaccini, Investigation of the mechanical properties of Mo-reinforced glass–matrix composites, J. Non-Cryst. Solids 344 (2004) 88–93.
[34] V. Cannillo, T. Manfredini, M. Montorsi, C. Siligardi, A. Sola, Microstructure-based modelling and experimental investigation of crack propagation in glass-alumina functionally graded materials, J. Eur. Ceram. Soc. 26 (15) (2006) 3067–3073.
[35] Z. Wang, A. Kulkarni, S. Deshpande, T. Nakamura, H. Herman, Effects of pores and interfaces on effective properties of plasma-sprayed zirconia coatings, Acta Mater. 51 (2003) 5319–5334.
[36] J. Gubicza, Determination of Young's modulus from depth sensing Vickers indentation tests, Solid State Phenom. 56 (1997) 195–200.
[37] W.C. Oliver, G.M. Pharr, An improved technique for determining hardness and elastic modulus using load and displacement sensing indentation experiments, J. Mater. Res. 7 (6) (1992) 1564–1583.